Structural Engineering and Mechanics, Vol. 6, No. 6 (1998) 643-658
DOI: http://dx.doi.org/10.12989/sem.1998.6.6.643

Thermal postbuckling of imperfect Reissner-Mindlin plates with two free side edges and resting on elastic foundations

Hui-Shen Shen†

Department of Civil Engineering, Shanghai Jiao Tong University, Shanghai 200030, China

Abstract. A thermal postbuckling analysis is presented for a moderately thick rectangular plate subjected to uniform or nonuniform tent-like temperature loading and resting on an elastic foundation. The plate is assumed to be simply supported on its two opposite edges and the two side edges remain free. The initial geometrical imperfection of the plate is taken into account. The formulation are based on the Reissner-Mindlin plate theory considering the first order shear deformation effect, and including plate-foundation interaction and thermal effects. The analysis uses a mixed Galerkin-perturbation technique to determine the thermal buckling loads and postbuckling equilibrium paths. Numerical examples are presented that relate to the performances of perfect and imperfect, moderately thick plates resting on Pasternak-type or softening nonlinear elastic foundations from which results for Winkler elastic foundations follow as a limiting case. Typical results are presented in dimensionless graphical form.

Key words: structural stability; thermal postbuckling; moderately thick plate; elastic foundation; Galerkin-perturbation method.

1. Introduction

In the thermal analysis of concrete pavements of roads and airfields, the problem is usually simplified and analyzed as moderately thick rectangular plates supported by an elastic foundation. These plates may have significant and unavoidable initial geometrical imperfections and are assumed to be simply supported on its two opposite edges and the two side edges remain free (see Harik *et al.* 1994). Due to boundary constraints, varying temperature environments typically induce stress, with ensuing buckling. Calculations of buckling behavior of such plates resting on elastic foundations are difficult problems and the difficulties increase when taking into account the large deflections of the plate.

Although a limited number of publications have appeared in the literature on the thermal buckling of thick plates subjected to temperature distribution, investigation of the thermal postbuckling response of thick plates is very limited. Thermal buckling loads for initially stressed transversely isotropic and antisymmetrically cross-ply laminated thick plates were evaluated using the Galerkin method by Chen *et al.* (1982) and by Yang and Shieh (1988). Thermal buckling analyses of composite laminated thick plates subjected to uniform or nonuniform temperature loading have been made by Tauchert (1987), Sun and Hsu (1990) and Chen *et al.* (1991).

† Professor

Noor and Peters (1992, 1994) and Noor *et al.* (1993) calculated buckling loads and postbuckling load-deflection curves of perfect, symmetrically laminated plates subjected to combined axial load and a uniform temperature distribution. Librescu and Souza (1993) analyzed postbuckling of an imperfect, shear-deformable, transversely isotropic plate under combined thermal and compressive edge loading. Shen and Zhu (1995) analyzed the thermal postbuckling of perfect and imperfect, moderately thick plates subjected to uniform or nonuniform tent-like temperature distribution using the deflection-type perturbation technique.

For elastic foundations, Raju and Rao (1988) calculated the thermal postbuckling response of a thin isotropic square plate resting on a Winkler elastic foundation by the finite element method. Dumir (1988) analyzed the thermal postbuckling of a thin isotropic rectangular plate resting on a Pasternak-type elastic foundation using the Galerkin method, but his numerical results were only for Winkler elastic foundation case. Recently, Shen *et al.* (1966) and Shen (1996a, b) analyzed the postbuckling of perfect and imperfect, thin and thick plates subjected to combined uniaxial compression and a uniform temperature distribution and resting on Pasternak-type or softening nonlinear elastic fouancations, from which results for Winkler elastic foundations follow as a limiting case.

Almost all of the investigations mentioned above are concerned with simply supported plates. Cui and Dowell (1983) considered the compressive postbuckling of perfect, orthotropic plates with two free side edges, but the analysis was limited to the thin plate. To the author's knowledge, there are no research works dealing with the thermal postbuckling of moderately thick plates with two free side edges subjected to nonuniform temperature loading and resting on elastic foundations, specially for imperfect ones.

Therefore, the present work focuses attention on the thermal postbuckling of moderately thick plates with two free side edges subjected to uniform or nonuniform tent-like temperature loading and resting on elastic foundations. Two types of foundation model are considered, i.e., Pasternak-type elastic foundation and softening nonlinear elastic foundation. The initial geometrical imperfection of the plate is taken into account. The material properties are assumed to be independent of temperature. The formulations are based on the Reissner-Mindlin plate theory considering the first order shear deformation effect, and including plate-foundation interaction and thermal effects. The analysis uses a mixed Galerkin-perturbation technique to determine the thermal buckling loads and postbuckling equilibrium paths.

2. Analytical formulation

Consider a moderately thick rectangular plate of length a, width b and thickness t simply supported on its two opposite edges and the two side edges remain free. The plate is subjected to thermal loading and rests on an elastic foundation. The foundation is assumed to be an attached foundation, that means no part of the plate lifts off the foundation in the postbuckled regime. The load-displacement relationship of the foundation is assumed to be $p=\overline{K}_1\overline{W}-\overline{K}_2\nabla^2\overline{W}-\overline{K}_3\overline{W}^3$, where p is the force per unit area, ∇^2 is the Laplace operator in X and Y, and $\overline{K}_1$, $\overline{K}_2$ and $\overline{K}_3$ are the Winkler, Pasternak and softening nonlinear elastic foundation stiffnesses, respectively. If $\overline{K}_3=0$, gives a Pasternak-type elastic foundation, and if $\overline{K}_2=0$ gives a softening nonlinear elastic foundation, as used for imperfect columns by Amazigo *et al.* (1970). Let $\overline{U}$, $\overline{V}$ and $\overline{W}$ be the plate displacements parallel to a right-hand set of axes (X, Y, Z), where X is longitudinal and Z is perpendicular to the plate. $\overline{\Psi}_x$ and $\overline{\Psi}_y$ are the mid-plane rotations of the normals about the Y and X axes, respectively. Denoting the initial deflection by $\overline{W}^*(X, Y)$, let $\overline{W}(X, Y)$ be the additional deflection, and $\overline{F}(X, Y)$ be the stress function for the stress resultants, and denoting differentiation by a comma, so that $N_x=\overline{F}_{,yy}$, $N_y=\overline{F}_{,xx}$ and $N_{xy}=-\overline{F}_{,xy}$.

From the Reissner-Mindlin plate theory considering the first order shear deformation effect, including plate-foundation interaction and thermal effects, the governing differential equations of such plates are

$$D\nabla^4\overline{W}+\nabla^2M^T=\left(1-\frac{D}{\kappa^2Gt}\nabla^2\right)[L(\overline{W}+\overline{W}^*,\overline{F})-(\overline{K}_1\overline{W}-\overline{K}_2\nabla^2\overline{W}-\overline{K}_3\overline{W}^3)] \tag{1}$$

$$\nabla^4\overline{F}+(1-\nu)\nabla^2N^T=-\frac{1}{2}EtL(\overline{W}+2\overline{W}^*,\overline{W}) \tag{2}$$

where

$$\nabla^4=\frac{\partial^4}{\partial X^4}+2\frac{\partial^4}{\partial X^2\partial Y^2}+\frac{\partial^4}{\partial Y^4}$$

$$\nabla^2=\frac{\partial^2}{\partial X^2}+\frac{\partial^2}{\partial Y^2}$$

$$L(\ )=\frac{\partial^2}{\partial X^2}\frac{\partial^2}{\partial Y^2}-2\frac{\partial^2}{\partial X\partial Y}\frac{\partial^2}{\partial X\partial Y}+\frac{\partial^2}{\partial Y^2}\frac{\partial^2}{\partial X^2}$$

in which D is flexural rigidity and $D=Et^3/12(1-\nu^2)$. E is Young's modulus, G is the in-plane shear modulus and ν is Poisson's ratio. Also κ^2 is the shear factor which accounts the non-uniformly of the shear strain distribution through the plate thickness, and for Reissner plate theory $\kappa^2=5/6$ while for Mindlin plate theory $\kappa^2=\pi^2/12$.

The nonuniform tent-like temperature rise is

$$T(X,Y,Z)=\begin{cases}T_0+2T_1Y/b & 0\le Y\le b/2\\ T_0+2T_1(1-Y/b) & b/2\le Y\le b\end{cases} \tag{3}$$

where T_0 is the uniform temperature rise, and T_1 is the temperature gradient.

The thermal force and moment are defined by

$$(N^T,M^T)=\frac{E\alpha}{1-\nu}\int_{-t/2}^{+t/2}(1,Z)T(X,Y,Z)\,dZ \tag{4}$$

in which α is thermal expansion coefficient for a plate. Because of Eqs. (3) and (4), it is noted that the thermal moment $M^T=0$ and $\nabla^2N^T=0$.

The unit end-shortening relationship is

$$\frac{\Delta_x}{a}=-\frac{1}{abt}\int_{-t/2}^{+t/2}\int_{-b/2}^{+b/2}\int_0^{\alpha}\frac{\partial\overline{U}}{\partial X}\,dXdYdZ$$

$$=-\frac{1}{ab}\int_{-b/2}^{+b/2}\int_0^{\alpha}\left[\frac{1}{Et}\left(\frac{\partial^2\overline{F}}{\partial Y^2}-\nu\frac{\partial^2\overline{F}}{\partial X^2}\right)-\frac{1}{2}\left(\frac{\partial\overline{W}}{\partial X}\right)^2-\frac{\partial\overline{W}}{\partial X}\frac{\partial\overline{W}^*}{\partial X}+\frac{1}{Et}(1-\nu)N^T\right]dXdY \tag{5}$$

If the plate is simply supported on its two opposite edges which is assumed to be restrained against expansion in the X-direction, and the two side edges remain free, the boundary conditions are

$X=0, a$;

$$\overline{W}=\overline{\Psi}_y=N_{xy}=0 \tag{6a}$$

$$\overline{M}_x=D\left(\frac{\partial\overline{\Psi}_x}{\partial X}+\nu\frac{\partial\overline{\Psi}_y}{\partial Y}\right)+M^T=0 \tag{6b}$$

$$\overline{U}=0 \tag{6c}$$

$Y=\pm b/2$;

$$\overline{M}_y=D\left(\nu\frac{\partial\overline{\Psi}_x}{\partial X}+\frac{\partial\overline{\Psi}_y}{\partial Y}\right)+M^T=0$$

$$\overline{M}_{xy}=\frac{1-\nu}{2}D\left(\frac{\partial\overline{\Psi}_x}{\partial Y}+\frac{\partial\overline{\Psi}_y}{\partial X}\right)=0 \tag{6e}$$

$$\overline{Q}_y=\kappa^2Gt\left(\overline{\Psi}_y+\frac{\partial\overline{W}}{\partial Y}\right)=0 \tag{6f}$$

$$\int_0^{\alpha}N_y\,dX=0 \tag{6g}$$

where $\overline{M}_x$ and $\overline{M}_y$ are, respectively, the bending moments per unit width and per unit length of the plate, and $\overline{Q}_y$ is the transverse shear force.

Eqs. (1)-(6) are the governing equations describing the required large deflection thermal postbuckling response of the plate.

3. Analytical method and asymptotic solutions

Let $\overline{\Phi}=\overline{\Psi}_{x,y}-\overline{\Psi}_{y,x}$ and $\lambda_T=12(1-\nu^2)b^2\alpha T_i/\pi^2t^2$ (i=0 for uniform temperature distribution and otherwise i=1) and introducing the dimensionless quantities (in which the alternative forms k_1, k_2 and k_3 are not needed until the numerical examples are considered)

$$x=\pi X/a,\quad y=\pi Y/b,\quad \beta=a/b,\quad \gamma=\pi^2D/\kappa^2a^2Gt,\quad \Phi=\overline{\Phi}a^2[12(1-\nu^2)]^{1/2}/\pi^2t,$$
$$(W, W^*)=(\overline{W}, \overline{W}^*)[12(1-\nu^2)]^{1/2}/t,\quad F=\overline{F}/D,\quad Q_y=\overline{Q}_y a^3[12(1-\nu^2)]^{1/2}/\pi^3Dt,$$
$$(M_x, M_y, M_{xy})=(\overline{M}_x, \overline{M}_y, \overline{M}_{xy})a^2[12(1-\nu^2)]^{1/2}/\pi^2Dt,$$
$$(K_1, k_1)=(a^4, b^4)\overline{K}_1/\pi^4D,\quad (K_2, k_2)=(a^2, b^2)\overline{K}_2/\pi^2D,$$
$$(K_3, k_3)=(a^4, b^4)\overline{K}_3/\pi^4D,\quad \delta_x=(\Delta_x/a)\,12(1-\nu^2)b^2/\pi^2t^2 \tag{7}$$

enables the nonlinear Eqs. (1) and (2) to be written in dimensionless form as

$$\overline{\nabla}^4W+[1-\gamma\overline{\nabla}^2][K_1W-K_2\overline{\nabla}^2W-K_3W^3]=\beta^2[1-\gamma\overline{\nabla}^2]L(W+W^*, F) \tag{8}$$

$$\overline{\nabla}^4F=-\frac{1}{2}\beta^2L(W+2W^*, W) \tag{9}$$

where

$$\overline{\nabla}^4 = \frac{\partial^4}{\partial x^4} + 2\beta^2 \frac{\partial^4}{\partial x^2 \partial y^2} + \beta^4 \frac{\partial^4}{\partial y^4}$$

$$\overline{\nabla}^2 = \frac{\partial^2}{\partial x^2} + \beta^2 \frac{\partial^2}{\partial y^2}$$

$$L(\ ) = \frac{\partial^2}{\partial x^2}\frac{\partial^2}{\partial y^2} - 2\frac{\partial^2}{\partial x \partial y}\frac{\partial^2}{\partial x \partial y} + \frac{\partial^2}{\partial y^2}\frac{\partial^2}{\partial x^2}$$

and the unit end-shortening relationship becomes

$$\delta_x = -\frac{1}{\pi^2 \beta^2}\int_{-\pi/2}^{+\pi/2}\int_0^{\pi}\left[\left(\beta^2 \frac{\partial^2 F}{\partial y^2} - \nu \frac{\partial^2 F}{\partial x^2}\right) - \frac{1}{2}\left(\frac{\partial W}{\partial x}\right)^2 - \frac{\partial W}{\partial x}\frac{\partial W^*}{\partial x} + \lambda_T \beta^2 C_{01}\right] dxdy \tag{10}$$

Note that in Eq. (10) for the uniform thermal loading case $C_{01}=1.0$ and $\lambda_T = 12(1-\nu^2)b^2\alpha T_0/\pi^2 t^2$, and for the nonuniform tent-like temperature loading case $C_{01}=(T_0/T_1+1/2)$ and $\lambda_T = 12(1-\nu^2)b^2\alpha T_1/\pi^2 t^2$.

The boundary conditions of Eq. (6) become

$x = 0, \pi$;

$$W = \Psi_y = F_{,xy} = M_x = 0 \tag{11a}$$

$$\delta_x = 0 \tag{11b}$$

$y = \pm\pi/2$;

$$M_y = -\overline{\nabla}^2 W + (1-\nu)\frac{\partial^2}{\partial x^2}[1+\gamma\overline{\nabla}^2]W - \frac{1}{2}(1-\nu)^2\gamma\beta\frac{\partial^2 \Phi}{\partial x \partial y} = 0 \tag{11c}$$

$$M_{xy} = -(1-\nu)\beta\frac{\partial^2}{\partial x \partial y}[1+\gamma\overline{\nabla}^2]W + \frac{1}{2}(1-\nu)\left[1-(1-\nu)\gamma\frac{\partial^2}{\partial x^2}\right]\Phi = 0 \tag{11d}$$

$$Q_y = -\beta\frac{\partial}{\partial y}\overline{\nabla}^2 W - \frac{1}{2}(1-\nu)\frac{\partial \Phi}{\partial x} = 0 \tag{11e}$$

$$\int_0^{\pi}\frac{\partial^2 F}{\partial x^2}dx = 0 \tag{11f}$$

Applying Eqs. (8)-(11), the thermal postbuckling behavior of Reissner-Mindlin plate is now determined by a mixed Galerkin-perturbation technique (see Shen and Lin 1995). The essence of this procedure, in the present case, is to assume that

$$W(x,y,\varepsilon) = \sum_{j=1}\varepsilon^j w_j(x,y), \qquad F(x,y,\varepsilon) = \sum_{j=0}\varepsilon^j f_j(x,y),$$

$$\Phi(x,y,\varepsilon) = \sum_{j=1}\varepsilon^j \phi_j(x,y) \tag{12}$$

where ε is a small perturbation parameter.

From Lévy-type solutions (see Nosier and Reddy 1992), the first term of $w_j(x, y)$ is assumed to have the form

$$w_1(x,y) = A_{11}^{(1)}\sin mx \operatorname{ch}\mu_1 y + A_{12}^{(1)}\sin mx \operatorname{ch}\mu_2 y \tag{13}$$

in which m is the number of half-waves in the X-direction and

$$\mu_{1,2}\beta=\left\{\left(m^2+\frac{K_2-\gamma(S_0m^2-K_1)}{2(1+\gamma K_2)}\right)\pm\left[\left(\frac{K_2-\gamma(S_0m^2-K_1)}{2(1+\gamma K_2)}\right)^2+\frac{S_0m^2-K_1}{1+\gamma K_2}\right]^{1/2}\right\}^{1/2} \tag{14}$$

where S_0 and $\lambda_T^{(0)}$ and $\lambda_T^{(2)}$ of Eq. (19) below are given in detail in the Appendix.

The initial geometrical imperfection is assumed to have a similar form to $W(x, y, \varepsilon)$, i.e.,

$$W^*(x, y, \varepsilon)=\mu W(x, y, \varepsilon) \tag{15}$$

where μ is the imperfection parameter.

Substituting Eq. (12) into Eqs. (8) and (9) gives a set of perturbation equations which can be solved step by step. At each step the amplitudes in terms of $w_j(x, y)$, $f_j(x, y)$ and $\phi_j(x, y)$ can be determined by the Galerkin procedure. As a result, the asymptotic solutions are obtained as

$$\begin{aligned}W=&\varepsilon[A_{11}^{(1)}\sin mx\,\mathrm{ch}\,\mu_1 y+A_{12}^{(1)}\sin mx\,\mathrm{ch}\,\mu_2 y]+\varepsilon^3[A_{11}^{(3)}\sin mx\,\mathrm{ch}\,\mu_1 y+A_{12}^{(3)}\sin mx\,\mathrm{ch}\,\mu_2 y\\&+A_{13}^{(3)}\sin mx\,\mathrm{ch}(2\mu_1+\mu_2)y+A_{14}^{(3)}\sin mx\,\mathrm{ch}(\mu_1+2\mu_2)y+A_{15}^{(3)}\sin mx\,\mathrm{ch}(2\mu_1-\mu_2)y\\&+A_{16}^{(3)}\sin mx\,\mathrm{ch}(\mu_1-2\mu_2)y+A_{17}^{(3)}\sin mx\,\mathrm{ch}3\mu_1 y+A_{18}^{(3)}\sin mx\,\mathrm{ch}3\mu_2 y\\&+A_{31}^{(3)}\sin 3mx\,\mathrm{ch}\,\mu_1 y+A_{32}^{(3)}\sin 3mx\,\mathrm{ch}\,\mu_2 y+A_{33}^{(3)}\sin 3mx\,\mathrm{ch}(2\mu_1+\mu_2)y\\&+A_{34}^{(3)}\sin 3mx\,\mathrm{ch}(\mu_1+2\mu_2)y+A_{35}^{(3)}\sin 3mx\,\mathrm{ch}(2\mu_1-\mu_2)y+A_{36}^{(3)}\sin 3mx\,\mathrm{ch}(\mu_1-2\mu_2)y\\&+A_{37}^{(3)}\sin 3mx\,\mathrm{ch}3\mu_1 y+A_{38}^{(3)}\sin 3mx\,\mathrm{ch}3\mu_2 y]+O(\varepsilon^4)\end{aligned} \tag{16}$$

$$\begin{aligned}F=&-B_{00}^{(0)}\frac{y^2}{2}+\varepsilon^2[-B_{00}^{(2)}\frac{y^2}{2}+B_{20}^{(2)}\cos 2mx+B_{02}^{(2)}\mathrm{ch}2\mu_1 y+b_{02}^{(2)}\mathrm{ch}2\mu_2 y\\&+B_{01}^{(2)}\mathrm{ch}(\mu_1+\mu_2)y+b_{01}^{(2)}\mathrm{ch}(\mu_1-\mu_2)y+B_{21}^{(2)}\cos 2mx\,\mathrm{ch}(\mu_1+\mu_2)y\\&+b_{21}^{(2)}\cos 2mx\,\mathrm{ch}(\mu_1-\mu_2)y]+O(\varepsilon^4)\end{aligned} \tag{17}$$

$$\begin{aligned}\Phi=&\varepsilon[C_{11}^{(1)}\cos mx\,\mathrm{sh}\,\mu_1 y+C_{12}^{(1)}\cos mx\,\mathrm{sh}\,\mu_2 y]+\varepsilon^3[C_{11}^{(3)}\cos mx\,\mathrm{sh}\,\mu_1 y+C_{12}^{(3)}\cos mx\,\mathrm{sh}\,\mu_2 y\\&+C_{13}^{(3)}\cos mx\,\mathrm{sh}(2\mu_1+\mu_2)y+C_{14}^{(3)}\cos mx\,\mathrm{sh}(\mu_1+2\mu_2)y+C_{15}^{(3)}\cos mx\,\mathrm{sh}(2\mu_1-\mu_2)y\\&+C_{16}^{(3)}\cos mx\,\mathrm{sh}(\mu_1-2\mu_2)y+C_{17}^{(3)}\cos mx\,\mathrm{sh}3\mu_1 y+C_{18}^{(3)}\cos mx\,\mathrm{sh}3\mu_2 y\\&+C_{31}^{(3)}\cos 3mx\,\mathrm{sh}\,\mu_1 y+C_{32}^{(3)}\cos 3mx\,\mathrm{sh}\,\mu_2 y+C_{33}^{(3)}\cos 3mx\,\mathrm{sh}(2\mu_1+\mu_2)y\\&+C_{34}^{(3)}\cos 3mx\,\mathrm{sh}(\mu_1+2\mu_2)y+C_{35}^{(3)}\cos 3mx\,\mathrm{sh}(2\mu_1-\mu_2)y+C_{36}^{(3)}\cos 3mx\,\mathrm{sh}(\mu_1-2\mu_2)y\\&+C_{37}^{(3)}\cos 3mx\,\mathrm{sh}3\mu_1 y+C_{38}^{(3)}\cos 3mx\,\mathrm{sh}3\mu_2 y]+O(\varepsilon^4)\end{aligned} \tag{18}$$

It is noted that Eqs. (16)-(18) satisfy boundary conditions (11a) and (11f) identically. By considering boundary conditions (11c)-(11e), all coefficients in Eqs. (16)-(18) are related and can be written as functions of $A_{11}^{(1)}$. Note that in Eqs. (16) and (18) the coefficients $A_{37}^{(3)}$, $A_{38}^{(3)}$, $C_{37}^{(3)}$ and $C_{38}^{(3)}$ are all zero for the case of Pasternak-type elastic foundation.

Next, substituting Eqs. (16) and (17) into boundary condition $\delta_x=0$, the thermal postbuckling equilibrium path can be written as

$$\lambda_T=\lambda_T^{(0)}+\lambda_T^{(2)}W_m^2+\cdots \tag{19}$$

in which W_m is the dimensionless form of the maximum deflection of the plate, which is assumed to be at the point $(x, y)=(\pi/2m, 0)$.

Eq. (19) can be employed to obtain numerical results for the thermal postbuckling load-

deflection curves of Reissner-Mindlin plates with two free side edges subjected to uniform or nonuniform tent-like thermal loading and resting on elastic foundations. The thermal buckling load of perfect plates can also readily be obtained numerically, by setting $\mu=0$ (or $\bar{W}^*/t=0$), while taking $W_m=0$ (or $\bar{W}/t=0$). In all cases, the minimum buckling load is determined by considering Eq. (19) for various values of m which determine the number of half-waves in the X-direction. From the Appendix, it can be seen that $\lambda_T^{(0)}$ is independent of the foundation stiffness K_3, so that the thermal buckling loads for Winkler and softening nonlinear elastic foundations are identical. As expected, the results of the next section show that K_3 affects the thermal postbuckling response of the plate, but does not affect its linear buckling load. In contrast, K_2 affects both the thermal buckling load and postbuckling response of the plate.

4. Numerical results and discussion

A thermal postbuckling analysis has been presented for a Reissner-Mindlin plate subjected to uniform or nonuniform tent-like thermal loads and resting on an elastic foundation. In the numerical analysis, asymptotic solutions up to 3rd-order were used. A number of examples were solved to illustrate their application to the performance of perfect and imperfect, moderately thick square plates simply supported on its two opposite edges and the two side edges remain free and resting on Pasternak-type or softening nonlinear elastic foundations. Throughout these numerical illustrations $\nu=0.3$, $\alpha=1.0\times10^{-5}/^{\circ}C$ and the transverse shear correction factor was considered $\kappa^2=\pi^2/12$. Typical results are presented in dimensionless graphical form. On all figures $\bar{W}^*/t$ and $\bar{W}/t$ mean the dimensionless forms of the maximum values of, respectively, the initial and additional deflection of the plate.

Fig. 1 gives the thermal postbuckling load-deflection curves of moderately thick square plates subjected to a uniform temperature rise and either without elastic foundations or resting on Winkler or Pasternak-type elastic foundations. The stiffnesses are $(k_1, k_2)=(2.0, 0.6)$ for the Pasternak-type elastic foundation, $(k_1, k_2)=(2.0, 0.0)$ for the Winkler elastic foundation, and $(k_1, k_2)=(0.0, 0.0)$ for the plate without any elastic foundation. It can be seen that the elastic foundation increases the thermal buckling load and it has a significant effect on thermal postbuckling behavior.

Fig. 2 gives the thermal postbuckling load-deflection curves of Reissner-Mindlin plates with

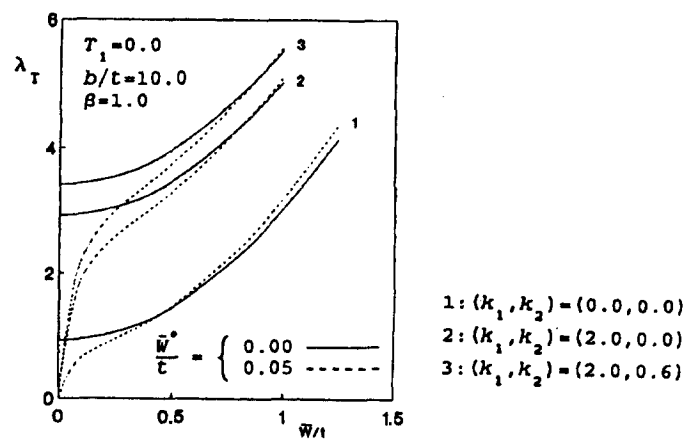

Fig. 1 Thermal postbuckling load-deflection curves of Reissner-Mindlin plates on Winkler or Pasternak-type elastic foundations or without elastic foundations

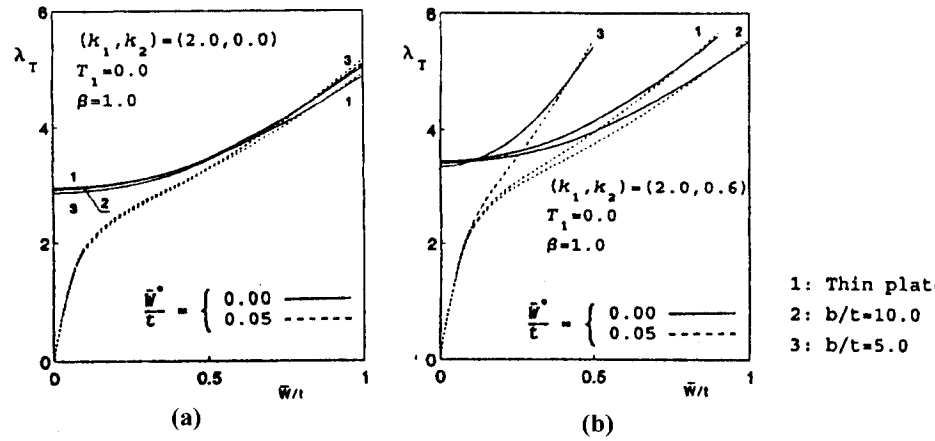

Fig. 2 Effect of transverse shear deformations on the thermal postbuckling of Reissner-Mindlin plates; (a) Winkler elastic foundation; (b) Pasternak-type elastic foundation

different thickness ratio b/t (=10.0, 5.0) subjected to uniform temperature loading and are compared with those of the thin plate. The results show that the thermal buckling load of the plate with b/t=5.0 is only about 2.9% lower than that of the thin plate in the case of Pasternak-type elastic foundation and is only about 3.1% lower than that of the thin plate in the case of Winkler elastic foundation, compare curves 1 and 3 in Fig. 2, so that the effect of transverse shear deformation on the thermal buckling load of the plate with two free side edges is rather less than that of the simply supported one (see Shen 1996a). It is found that the thermal buckling load and postbuckling strength are decreased by decreasing the plate b/t. The thermal postbuckling load-deflection curves of thick and thin plates differ substantially in the Pasternak-type elastic foundation case, but have minor difference in the Winkler elastic foundation case.

Fig. 3 shows the effect of thermal load ratio T_0/T_1 (=0.0, 0.5, 1.0) on the thermal postbuckling response of Reissner-Mindlin plates under nonuniform tent-like temperature

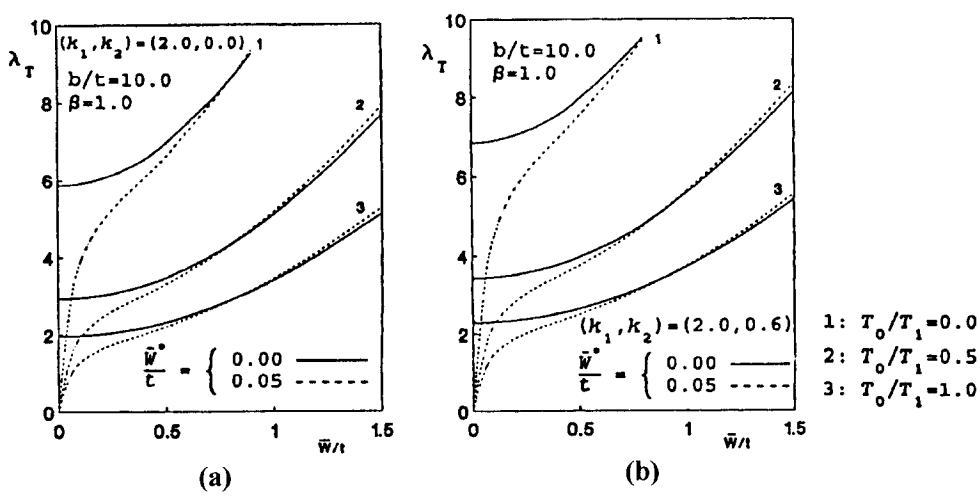

Fig. 3 Effect of thermal load ratio T_0/T_1 on the postbuckling of Reissner-Mindlin plates: (a) Winkler elastic foundation; (b) Pasternak-type elastic foundation

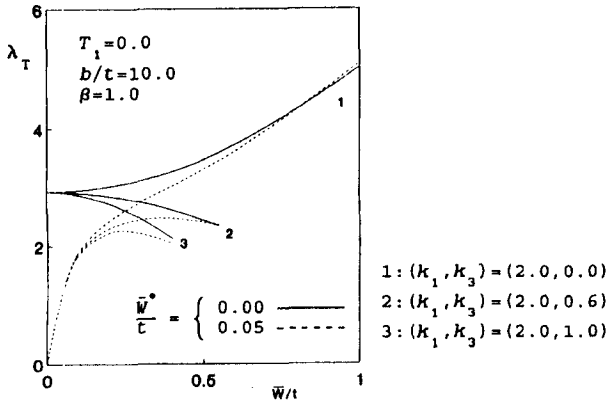

Fig. 4 Thermal postbuckling load-deflection curves of Reissner-Mindlin plates on Winkler or nonlinear elastic foundations

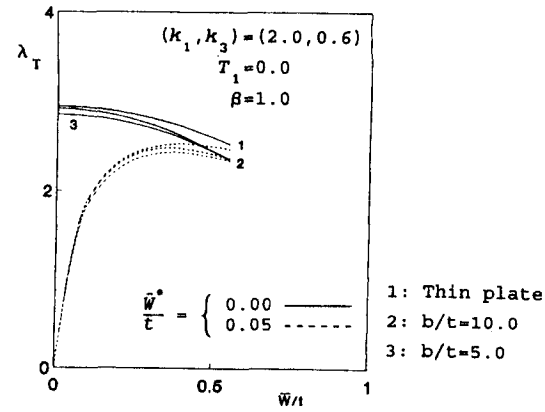

Fig. 5 Effect of transverse shear deformations on the thermal postbuckling of Reissner-Mindlin plates on nonlinear elastic foundations

loading and resting on Winkler or Pasternak-type elastic foundations. As expected, these results show that the thermal buckling load is decreased by increasing the thermal load ratio T_0/T_1 and that the thermal postbuckling equilibrium path becomes significantly lower as the thermal load ratio T_0/T_1 increases.

In Figs. 1 and 3, the plate thickness ratio b/t=10.0, and in Figs. 2 and 3 the Winkler and the Pasternak-type elastic foundation stiffnesses are characterized by (k_1, k_2)=(2.0, 0.0) and (2.0, 0.6), respectively.

Figs. 4-6 show thermal postbuckling results analogous to the results of Figs. 1-3, but are for the case of softening nonlinear elastic foundation. In Figs. 4-6 the nonlinear elastic foundation stiffness is characterized by (k_1, k_3)=(2.0, 0.6) or (2.0, 1.0). Note that now the thermal postbuckling equilibrium path is unstable and imperfection sensitivity can be predicted.

Fig. 7 shows the curves of imperfection sensitivity of thermally stressed Reissner-Mindlin plates resting on softening nonlinear elastic foundations. λ^* is the maximum value of λ_T and $\bar{W}/t$ varies on curves such as those of Figs. 4-6, made dimensionless by dividing by the critical value of λ_T for the perfect plate. These results show that the imperfection sensitivity of the

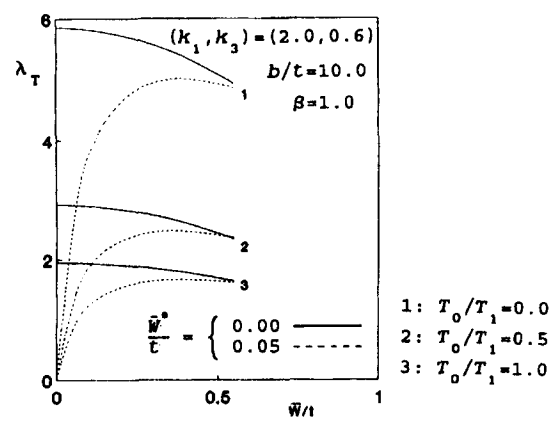

Fig. 6 Effect of thermal load ratio T_0/T_1 on the postbuckling of Reissner-Mindlin plates on nonlinear elastic foundations

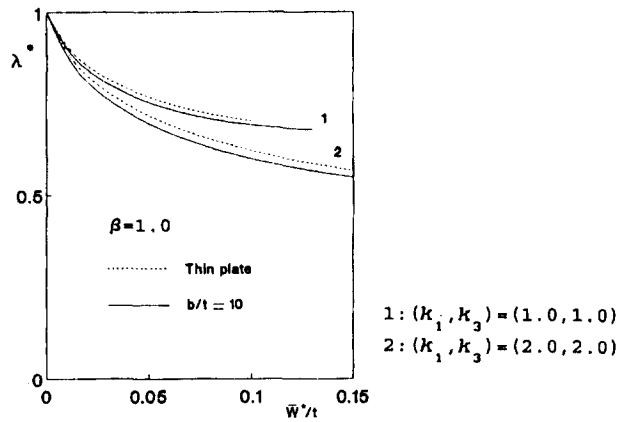

Fig. 7 Comparisons of curves of imperfection sensitivity of Reissner-Mindlin plates on nonlinear elastic foundations

plate on a nonlinear elastic foundation with (k_1, k_3)=(2.0, 2.0) is large and is considerably greater than that of the plate on a nonlinear elastic foundation with (k_1, k_3)=(1.0, 1.0). The results calculated show that the imperfection sensitivities are almost the same for the plate under either uniform or nonuniform temperature loading. Also the imperfection sensitivity of the moderately thick plate is slight greater than that of the thin plate. Note that because the reaction force p could be negative in the large deflection range, the results presented were only for small initial geometrical imperfections.

5. Conclusions

Thermal postbuckling of Reissner-Mindlin plates with two free side edges and resting on elastic foundations, induced by uniform or nonuniform tent-like temperature distribution, has been studied by a mixed Galerkin-perturbation method. The numerical examples presented relate to the performance of perfect and imperfect, moderately thick square plates resting on Winkler or Pasternak-type or softening nonlinear elatic foundations. They show that the thermal postbuckling responses for Winkler, Pasternak-type and softening nonlinear elastic foundation cases differ substantially. They also show that the characteristics of thermal postbuckling are significantly influenced by foundation stiffness, thermal load ratio and initial geometrical imperfection.

Unlike the plate resting on a Winkler or Pasternak-type elastic foundation, which has a stable postbuckling equilibrium path, the Reissner-Mindlin plate resting on a softening nonlinear elastic foundation has an unstable thermal postbuckling equilibrium configuration. For such cases, the plate is an imperfection-sensitive structure that exhibits all of the interesting features of such structures.

References

Amazigo, J.C., Budiansky, B. and Carrier, G.F. (1970), "Asymptotic analysis of the buckling of imperfect columns on nonlinear elastic foundation", *Int. J. Solids Structures*, **6**, 1341-1356.

Chen, L.W., Brunelle, E.J. and Chen, L.Y. (1982), "Thermal buckling of initial stressed thick plates", *J. Mech. Des.*, **104**, 557-564.

Chen, W.J., Lin, P.D. and Chen, L.W. (1991), "Thermal buckling behavior of thick composite laminated plates under nonuniform temperature distribution", *Comput. Struct.*, **41**, 637-645.
Cui, E.J. and Dowell, E.H. (1983), "Postbuckling behavior of rectangular orthotropic plates with two free side edges", *Int. J. Mech. Sci.*, **25**, 429-446.
Dumir, P.C. (1988), "Thermal postbuckling of rectangular plates on Pasternak elastic foundations", *Mech. Res. Communications*, **15**, 371-379.
Harik, I.E., Jianping, P., Southgate, H. and Allen, D. (1994), "Temperature effects on rigid pavements", *ASCE J. Transportation Engrg.*, **120**, 127-143.
Librescu, L. and Souza, M.A. (1993), "Post-buckling of geometrically imperfect shear-deformable flat panels under combined thermal and compressive edge loadings", *ASME J. Appl. Mech.*, **60**, 526-533.
Noor, A.K. and Peters, J.M. (1992), "Postbuckling of multilayered composite plates subjected to combined axial and thermal loads", *Finite Elements Anal. Des.*, **11**, 91-104.
Noor, A.K. and Peters, J.M. (1994), "Finite element buckling and postbuckling solutions for multilayered composite panels", *Finite Elements Anal. Des.*, **15**, 343-361.
Noor, A.K., Starnes, J.H. and Peters, J.M. (1993), "Thermomechanical buckling and postbuckling of multilayered composite panels", *Composite Struct.*, **23**, 233-251.
Nosier, A. and Reddy, J.N. (1992), "On vibration and buckling of symmetric laminated plates according to shear deformation theories. Part II", *Acta Mechanica*, **94**, 145-169.
Raju, K.K. and Rao, G.V. (1988), "Thermal post-buckling of a square plate resting on an elastic foundation by finite element method", *Comput. Struct.*, **28**, 195-199.
Shen, H.S. (1996a), "Thermomechanical postbuckling of imperfect moderately thick plates on two-parameter elastic fouincations", *Structural Engineering and Mechanics*, **4**, 149-162.
Shen, H.S. (1996b), "Thermomechanical postbuckling of imperfect moderately thick plates on nonlinear elastic fouincations", *Mechanics of Structures and Machines*, **24**, 513-530.
Shen, H.S. and Lin, Z.Q. (1995), "Thermal post-buckling analysis of imperfect laminated plates", *Comput. Struct.*, **57**, 533-540.
Shen, H.S., Sun, G. and Williams, F.W. (1996), "Thermomechanical postbuckling analysis of imperfect laminated plates on two-parameter elastic foundations", *Composite Struct.*, **34**, 325-338.
Shen, H.S. and Zhu, X.G. (1995), "Thermal postbuckling analysis of moderately thick plates", *Appl. Math. Mech.*, **16**, 475-484.
Sun, L.X. and Hsu, T.R. (1990), "Thermal buckling of laminated composite plates with transverse shear deformation", *Comput. Struct.*, **36**, 883-889.
Tauchert, T.R. (1987), "Thermal buckling of thick antisymmetric angle-ply laminates", *J. Therm. Stresses*, **10**, 113-124.
Yang, I.H. and Shieh, J.A. (1988), "Generic thermal buckling of initial stressed antisymmetric cross-ply thick laminates", *Int. J. Solids Struct.*, **24**, 1059-1070.

Appendix

In Eq. (19)

$$(\lambda_T^{(0)}, \lambda_T^{(2)}) = (S_0, S_2)/((1+\mu)\beta^2 C_{01} \tag{20}$$

where S_0 is obtained from equation

$$\frac{\mu_1\beta[(2-\nu)m^2-\mu_1^2\beta^2]}{\nu m^2-\mu_1^2\beta^2+(1-\nu)\gamma(m^2-\mu_1^2\beta^2)^2}\,\text{th}\,\frac{\mu_1\pi}{2}-\frac{\mu_2\beta[(2-\nu)m^2-\mu_2^2\beta^2]}{\nu m^2-\mu_2^2\beta^2+(1-\nu)\gamma(m^2-\mu_2^2\beta^2)^2}\,\text{th}\,\frac{\mu_2\pi}{2}=0 \tag{21}$$

and

$$S_2=\frac{C_{20}}{m^2C_{02}}+\frac{1}{8}m^2(1+\alpha_{112}^2)(1+\mu)(1+2\mu)$$

$$C_{02}=[1+\gamma(m^2-\mu_1^2\beta^2)]\left[\left(1+\frac{1}{\mu_1\pi}\,\mathrm{sh}\mu_1\pi\right)\alpha_{311}+\left(\frac{2}{(\mu_1+\mu_2)\pi}\,\mathrm{sh}\,\frac{(\mu_1+\mu_2)\pi}{2}\right.\right.$$

$$\left.\left.+\frac{2}{(\mu_1-\mu_2)\pi}\,\mathrm{sh}\,\frac{(\mu_1-\mu_2)\pi}{2}\right)\alpha_{312}\right]+[1+\gamma(m^2-\mu_2^2\beta^2)]\left[\left(\frac{2}{(\mu_1+\mu_2)\pi}\,\mathrm{sh}\,\frac{(\mu_1+\mu_2)\pi}{2}\right.\right.$$

$$\left.\left.+\frac{2}{(\mu_1-\mu_2)\pi}\,\mathrm{sh}\,\frac{(\mu_1-\mu_2)\pi}{2}\right)\alpha_{311}+\left(1+\frac{1}{\mu_2\pi}\,\mathrm{sh}\mu_2\pi\right)\alpha_{312}\right]\alpha_{112}$$

$$C_{20}=(g_{111}\alpha_{311}^2+C_{22}\alpha_{311}+g_{331}\alpha_{331}^2-C_{26}\alpha_{331})\left(1+\frac{1}{\mu_1\pi}\,\mathrm{sh}\mu_1\pi\right)$$

$$+(g_{112}\alpha_{312}^2+C_{24}\alpha_{312}+g_{332}\alpha_{332}^2-C_{28}\alpha_{332})\left(1+\frac{1}{\mu_2\pi}\,\mathrm{sh}\mu_2\pi\right)$$

$$+(g_{111}\alpha_{311}\alpha_{312}+C_{22}\alpha_{312}+g_{112}\alpha_{311}\alpha_{312}+C_{24}\alpha_{311}+g_{331}\alpha_{331}\alpha_{332}$$

$$-C_{26}\alpha_{332}+g_{332}\alpha_{331}\alpha_{332}-C_{28}\alpha_{331})\left(\frac{2}{(\mu_1+\mu_2)\pi}\,\mathrm{sh}\,\frac{(\mu_1+\mu_2)\pi}{2}+\frac{2}{(\mu_1-\mu_2)\pi}\,\mathrm{sh}\,\frac{(\mu_1-\mu_2)\pi}{2}\right)$$

$$C_{22}=\frac{1}{16}[1+\gamma(m^2-\mu_1^2\beta^2)]\left\{\left[m^4(1+4\alpha_{112}^2)+\frac{m^4(\mu_1-\mu_2)^4\beta^4}{[4m^2-(\mu_1+\mu_2)^2\beta^2]^2}\alpha_{112}^2\right.\right.$$

$$\left.\left.+\frac{m^4(\mu_1+\mu_2)^4\beta^4}{[4m^2-(\mu_1-\mu_2)^2\beta^2]^2}\alpha_{112}^2+\mu_1^2\beta^2(\mu_1^2\beta^2+\mu_2^2\beta^2\alpha_{112}^2)\right](1+\mu)(1+2\mu)-9K_3(1+2\alpha_{112}^2)\right\}$$

$$C_{24}=\frac{1}{16}[1+\gamma(m^2-\mu_2^2\beta^2)]\left\{\left[m^4(\alpha_{112}^2+4)+\frac{m^4(\mu_1-\mu_2)^4\beta^4}{[4m^2-(\mu_1+\mu_2)^2\beta^2]^2}\right.\right.$$

$$\left.\left.+\frac{m^4(\mu_1+\mu_2)^4\beta^4}{[4m^2-(\mu_1-\mu_2)^2\beta^2]^2}+\mu_2^2\beta^2(\mu_1^2\beta^2+\mu_2^2\beta^2\alpha_{112}^2)\right](1+\mu)(1+2\mu)-9K_3(\alpha_{112}^2+2)\right\}\alpha_{112}$$

$$C_{26}=\frac{1}{16}[1+\gamma(9m^2-\mu_1^2\beta^2)]\left\{\left[\frac{m^4(\mu_1-\mu_2)^2(\mu_1+3\mu_2)^2\beta^4}{[4m^2-(\mu_1+\mu_2)^2\beta^2]^2}\alpha_{112}^2\right.\right.$$

$$\left.\left.+\frac{m^4(\mu_1+\mu_2)^2(\mu_1-3\mu_2)^2\beta^4}{[4m^2-(\mu_1-\mu_2)^2\beta^2]^2}\alpha_{112}^2+\mu_1^2\beta^2(\mu_1^2\beta^2+\mu_2^2\beta^2\alpha_{112}^2)\right](1+\mu)(1+2\mu)-3K_3(1+2\alpha_{112}^2)\right\}$$

$$C_{28}=\frac{1}{16}[1+\gamma(9m^2-\mu_2^2\beta^2)]\left\{\left[\frac{m^4(\mu_1-\mu_2)^2(3\mu_1+\mu_2)^2\beta^4}{[4m^2-(\mu_1+\mu_2)^2\beta^2]^2}+\frac{m^4(\mu_1+\mu_2)^2(3\mu_1-\mu_2)^2\beta^4}{[4m^2-(\mu_1-\mu_2)^2\beta^2]^2}\right.\right.$$

$$+\mu_2^2\beta^2(\mu_1^2\beta^2+\mu_2^2\beta^2\alpha_{112}^2)\Big](1+\mu)(1+2\mu)-3K_3(\alpha_{112}^2+2)\Big\}\alpha_{112}$$

$$\alpha_{112}=-\frac{\nu m^2-\mu_1^2\beta^2+(1-\nu)\gamma(m^2-\mu_1^2\beta^2)^2}{\nu m^2-\mu_2^2\beta^2+(1-\nu)\gamma(m^2-\mu_2^2\beta^2)^2}\frac{\operatorname{ch}\dfrac{\mu_1\pi}{2}}{\operatorname{ch}\dfrac{\mu_2\pi}{2}}$$

$$\alpha_{313}=-\frac{1}{16g_{313}}[1+\gamma(m^2-(2\mu_1+\mu_2)^2\beta^2)]\left\{\left[3m^4+\frac{m^4(\mu_1-\mu_2)^2(3\mu_1+\mu_2)^2\beta^4}{[4m^2-(\mu_1+\mu_2)^2\beta^2]^2}\right]\right.$$
$$\left.\times(1+\mu)(1+2\mu)-9K_3\right\}\alpha_{112}$$

$$\alpha_{314}=-\frac{1}{16g_{314}}[1+\gamma(m^2-(\mu_1+2\mu_2)^2\beta^2)]\left\{\left[3m^4+\frac{m^4(\mu_1-\mu_2)^2(\mu_1+3\mu_2)^2\beta^4}{[4m^2-(\mu_1+\mu_2)^2\beta^2]^2}\right]\right.$$
$$\left.\times(1+\mu)(1+2\mu)-9K_3\right\}\alpha_{112}^2$$

$$\alpha_{315}=-\frac{1}{16g_{315}}[1+\gamma(m^2-(2\mu_1-\mu_2)^2\beta^2)]\left\{\left[3m^4+\frac{m^4(\mu_1+\mu_2)^2(3\mu_1-\mu_2)^2\beta^4}{[4m^2-(\mu_1-\mu_2)^2\beta^2]^2}\right]\right.$$
$$\left.\times(1+\mu)(1+2\mu)-9K_3\right\}\alpha_{112}$$

$$\alpha_{316}=-\frac{1}{16g_{316}}[1+\gamma(m^2-(\mu_1-2\mu_2)^2\beta^2)]\left\{\left[3m^4+\frac{m^4(\mu_1+\mu_2)^2(\mu_1-3\mu_2)^2\beta^4}{[4m^2-(\mu_1-\mu_2)^2\beta^2]^2}\right]\right.$$
$$\left.\times(1+\mu)(1+2\mu)-9K_3\right\}\alpha_{112}^2$$

$$\alpha_{317}=-\frac{1}{16g_{317}}[1+\gamma(m^2-9\mu_1^2\beta^2)][m^4(1+\mu)(1+2\mu)-3K_3]$$

$$\alpha_{318}=-\frac{1}{16g_{318}}[1+\gamma(m^2-9\mu_2^2\beta^2)][m^4(1+\mu)(1+2\mu)-3K_3]\alpha_{112}^3$$

$$\alpha_{333}=\frac{1}{16g_{333}}[1+\gamma(9m^2-(2\mu_1+\mu_2)^2\beta^2)]\left[\frac{m^4(\mu_1-\mu_2)^4\beta^4}{[4m^2-(\mu_1+\mu_2)^2\beta^2]^2}(1+\mu)(1+2\mu)-3K_3\right]\alpha_{112}$$

$$\alpha_{334}=\frac{1}{16g_{334}}[1+\gamma(9m^2-(\mu_1+2\mu_2)^2\beta^2)]\left[\frac{m^4(\mu_1-\mu_2)^4\beta^4}{[4m^2-(\mu_1+\mu_2)^2\beta^2]^2}(1+\mu)(1+2\mu)-3K_3\right]\alpha_{112}^2$$

$$\alpha_{335}=\frac{1}{16g_{335}}[1+\gamma(9m^2-(2\mu_1-\mu_2)^2\beta^2)]\left[\frac{m^4(\mu_1+\mu_2)^4\beta^4}{[4m^2-(\mu_1-\mu_2)^2\beta^2]^2}(1+\mu)(1+2\mu)-3K_3\right]\alpha_{112}$$

$$\alpha_{336}=\frac{1}{16g_{336}}[1+\gamma(9m^2-(\mu_1-2\mu_2)^2\beta^2)]\left[\frac{m^4(\mu_1+\mu_2)^4\beta^4}{[4m^2-(\mu_1-\mu_2)^2\beta^2]^2}(1+\mu)(1+2\mu)-3K_3\right]\alpha_{112}^2$$

$$\alpha_{337}=-\frac{K_3}{16g_{337}}[1+9\gamma(m^2-\mu_1^2\beta^2)]$$

$$\alpha_{338}=-\frac{K_3}{16g_{338}}[1+9\gamma(m^2-\mu_2^2\beta^2)]$$

$$\alpha_{311}=-\frac{c_3c_5-c_2c_6}{c_1c_5-c_2c_4},\qquad \alpha_{312}=-\frac{c_1c_6-c_3c_4}{c_1c_5-c_2c_4}$$

$$c_1=[\nu m^2-\mu_1^2\beta^2+(1-\nu)\gamma(m^2-\mu_1^2\beta^2)^2]\,\mathrm{ch}\,\frac{\mu_1\pi}{2}$$

$$c_2=[\nu m^2-\mu_2^2\beta^2+(1-\nu)\gamma(m^2-\mu_2^2\beta^2)^2]\,\mathrm{ch}\,\frac{\mu_2\pi}{2}$$

$$c_3=\alpha_{313}\{\nu m^2-(2\mu_1+\mu_2)^2\beta^2+(1-\nu)\gamma[m^2-(2\mu_1+\mu_2)^2\beta^2]^2\}\,\mathrm{ch}\,\frac{(2\mu_1+\mu_2)\pi}{2}$$
$$+\alpha_{314}\{\nu m^2-(\mu_1+2\mu_2)^2\beta^2+(1-\nu)\gamma[m^2-(\mu_1+2\mu_2)^2\beta^2]^2\}\,\mathrm{ch}\,\frac{(\mu_1+2\mu_2)\pi}{2}$$
$$+\alpha_{315}\{\nu m^2-(2\mu_1-\mu_2)^2\beta^2+(1-\nu)\gamma[m^2-(2\mu_1-\mu_2)^2\beta^2]^2\}\,\mathrm{ch}\,\frac{(2\mu_1-\mu_2)\pi}{2}$$
$$+\alpha_{316}\{\nu m^2-(\mu_1-2\mu_2)^2\beta^2+(1-\nu)\gamma[m^2-(\mu_1-2\mu_2)^2\beta^2]^2\}\,\mathrm{ch}\,\frac{(\mu_1-2\mu_2)\pi}{2}$$
$$+\alpha_{317}[\nu m^2-9\mu_1^2\beta^2+(1-\nu)\gamma(m^2-9\mu_1^2\beta^2)^2]\,\mathrm{ch}\,\frac{3\mu_1\pi}{2}$$
$$+\alpha_{318}[\nu m^2-9\mu_2^2\beta^2+(1-\nu)\gamma(m^2-9\mu_2^2\beta^2)^2]\,\mathrm{ch}\,\frac{3\mu_2\pi}{2}$$

$$c_4=\mu_1\beta[(2-\nu)m^2-\mu_1^2\beta^2]\,\mathrm{sh}\,\frac{\mu_1\pi}{2}$$

$$c_5=\mu_2\beta[(2-\nu)m^2-\mu_2^2\beta^2]\,\mathrm{sh}\,\frac{\mu_2\pi}{2}$$

$$c_6=\alpha_{313}(2\mu_1+\mu_2)\beta[(2-\nu)m^2-(2\mu_1+\mu_2)^2\beta^2]\,\mathrm{sh}\,\frac{(2\mu_1+\mu_2)\pi}{2}$$
$$+\alpha_{314}(\mu_1+2\mu_2)\beta[(2-\nu)m^2-(\mu_1+2\mu_2)^2\beta^2]\,\mathrm{sh}\,\frac{(\mu_1+2\mu_2)\pi}{2}$$
$$+\alpha_{315}(2\mu_1-\mu_2)\beta[(2-\nu)m^2-(2\mu_1-\mu_2)^2\beta^2]\,\mathrm{sh}\,\frac{(2\mu_1-\mu_2)\pi}{2}$$
$$+\alpha_{316}(\mu_1-2\mu_2)\beta[(2-\nu)m^2-(\mu_1-2\mu_2)^2\beta^2]\,\mathrm{sh}\,\frac{(\mu_1-2\mu_2)\pi}{2}$$
$$+\alpha_{317}\mu_1\beta[(2-\nu)m^2-9\mu_1^2\beta^2]\,\mathrm{sh}\,\frac{3\mu_1\pi}{2}$$
$$+\alpha_{318}\mu_2\beta[(2-\nu)m^2-9\mu_2^2\beta^2]\,\mathrm{sh}\,\frac{3\mu_2\pi}{2}$$

$$\alpha_{331}=-\frac{c_9c_{11}-c_8c_{12}}{c_7c_{11}-c_8c_{10}},\qquad \alpha_{332}=-\frac{c_7c_{12}-c_9c_{10}}{c_7c_{11}-c_8c_{10}}$$

$$c_7=[9\nu m^2-\mu_1^2\beta^2+(1-\nu)\gamma(9m^2-\mu_1^2\beta^2)^2]\,\mathrm{ch}\,\frac{\mu_1\pi}{2}$$

$$c_8=[9\nu m^2-\mu_2^2\beta^2+(1-\nu)\gamma(9m^2-\mu_2^2\beta^2)^2]\,\mathrm{ch}\,\frac{\mu_2\pi}{2}$$

$$c_9=\alpha_{333}\{9\nu m^2-(2\mu_1+\mu_2)^2\beta^2+(1-\nu)\gamma[9m^2-(2\mu_1+\mu_2)^2\beta^2]^2\}\,\mathrm{ch}\,\frac{(2\mu_1+\mu_2)\pi}{2}$$

$$+\alpha_{334}\{9\nu m^2-(\mu_1+2\mu_2)^2\beta^2+(1-\nu)\gamma[9m^2-(\mu_1+2\mu_2)^2\beta^2]^2\}\ \mathrm{ch}\frac{(\mu_1+2\mu_2)\pi}{2}$$

$$+\alpha_{335}\{9\nu m^2-(2\mu_1-\mu_2)^2\beta^2+(1-\nu)\gamma[9m^2-(2\mu_1-\mu_2)^2\beta^2]^2\}\ \mathrm{ch}\frac{(2\mu_1-\mu_2)\pi}{2}$$

$$+\alpha_{336}\{9\nu m^2-(\mu_1-2\mu_2)^2\beta^2+(1-\nu)\gamma[9m^2-(\mu_1-2\mu_2)^2\beta^2]^2\}\ \mathrm{ch}\frac{(\mu_1-2\mu_2)\pi}{2}$$

$$+9\alpha_{337}[\nu m^2-\mu_1^2\beta^2+(1-\nu)\gamma(m^2-\mu_1^2\beta^2)^2]\ \mathrm{ch}\frac{3\mu_1\pi}{2}$$

$$+9\alpha_{338}[\nu m^2-\mu_2^2\beta^2+(1-\nu)\gamma(m^2-\mu_2^2\beta^2)^2]\ \mathrm{ch}\frac{3\mu_2\pi}{2}$$

$$c_{10}=\mu_1\beta[(2-\nu)9m^2-\mu_1^2\beta^2]\ \mathrm{sh}\frac{\mu_1\pi}{2}$$

$$c_{11}=\mu_2\beta[(2-\nu)9m^2-\mu_2^2\beta^2]\ \mathrm{sh}\frac{\mu_2\pi}{2}$$

$$c_{12}=\alpha_{333}(2\mu_1+\mu_2)\beta[(2-\nu)9m^2-(2\mu_1+\mu_2)^2\beta^2]\ \mathrm{sh}\frac{(2\mu_1+\mu_2)\pi}{2}$$

$$+\alpha_{334}(\mu_1+2\mu_2)\beta[(2-\nu)9m^2-(\mu_1+2\mu_2)^2\beta^2]\ \mathrm{sh}\frac{(\mu_1+2\mu_2)\pi}{2}$$

$$+\alpha_{335}(2\mu_1-\mu_2)\beta[(2-\nu)9m^2-(2\mu_1-\mu_2)^2\beta^2]\ \mathrm{sh}\frac{(2\mu_1-\mu_2)\pi}{2}$$

$$+\alpha_{336}(\mu_1-2\mu_2)\beta[(2-\nu)9m^2-(\mu_1-2\mu_2)^2\beta^2]\ \mathrm{sh}\frac{(\mu_1-2\mu_2)\pi}{2}$$

$$+27\alpha_{337}\mu_1\beta[(2-\nu)m^2-\mu_1^2\beta^2]\ \mathrm{sh}\frac{3\mu_1\pi}{2}$$

$$+27\alpha_{338}\mu_2\beta[(2-\nu)m^2-\mu_2^2\beta^2]\ \mathrm{sh}\frac{3\mu_2\pi}{2}$$

$$g_{111}=(m^2-\mu_1^2\beta^2)^2+[K_1+K_2(m^2-\mu_1^2\beta^2)-S_0m^2][1+\gamma(m^2-\mu_1^2\beta^2)]$$

$$g_{112}=(m^2-\mu_2^2\beta^2)^2+[K_1+K_2(m^2-\mu_2^2\beta^2)-S_0m^2][1+\gamma(m^2-\mu_2^2\beta^2)]$$

$$g_{313}=[m^2-(2\mu_1+\mu_2)^2\beta^2]^2+\{K_1+K_2[m^2-(2\mu_1+\mu_2)^2\beta^2]-S_0m^2\}[1+\gamma(m^2-(2\mu_1+\mu_2)^2\beta^2)]$$

$$g_{314}=[m^2-(\mu_1+2\mu_2)^2\beta^2]^2+\{K_1+K_2[m^2-(\mu_1+2\mu_2)^2\beta^2]-S_0m^2\}[1+\gamma(m^2-(\mu_1+2\mu_2)^2\beta^2)]$$

$$g_{315}=[m^2-(2\mu_1-\mu_2)^2\beta^2]^2+\{K_1+K_2[m^2-(2\mu_1-\mu_2)^2\beta^2]-S_0m^2\}[1+\gamma(m^2-(2\mu_1-\mu_2)^2\beta^2)]$$

$$g_{316}=[m^2-(\mu_1-2\mu_2)^2\beta^2]^2+\{K_1+K_2[m^2-(\mu_1-2\mu_2)^2\beta^2]-S_0m^2\}[1+\gamma(m^2-(\mu_1-2\mu_2)^2\beta^2)]$$

$$g_{317}=(m^2-9\mu_1^2\beta^2)^2+[K_1+K_2(m^2-9\mu_1^2\beta^2)-S_0m^2][1+\gamma(m^2-9\mu_1^2\beta^2)]$$

$$g_{318}=(m^2-9\mu_2^2\beta^2)^2+[K_1+K_2(m^2-9\mu_2^2\beta^2)-S_0m^2][1+\gamma(m^2-9\mu_2^2\beta^2)]$$

$$g_{331}=(9m^2-\mu_1^2\beta^2)^2+[K_1+K_2(9m^2-\mu_1^2\beta^2)-9S_0m^2][1+\gamma(9m^2-\mu_1^2\beta^2)]$$

$$g_{332}=(9m^2-\mu_2^2\beta^2)^2+[K_1+K_2(9m^2-\mu_2^2\beta^2)-9S_0m^2][1+\gamma(9m^2-\mu_2^2\beta^2)]$$

$$g_{333}=[9m^2-(2\mu_1+\mu_2)^2\beta^2]^2+\{K_1+K_2[9m^2-(2\mu_1+\mu_2)^2\beta^2]-9S_0m^2\}[1+\gamma(9m^2-(2\mu_1+\mu_2)^2\beta^2)]$$

$$g_{334}=[9m^2-(\mu_1+2\mu_2)^2\beta^2]^2+\{K_1+K_2[9m^2-(\mu_1+2\mu_2)^2\beta^2]-9S_0m^2\}[1+\gamma(9m^2-(\mu_1+2\mu_2)^2\beta^2)]$$

$$g_{335}=[9m^2-(2\mu_1-\mu_2)^2\beta^2]^2+\{K_1+K_2[9m^2-(2\mu_1-\mu_2)^2\beta^2]-9S_0m^2\}[1+\gamma(9m^2-(2\mu_1-\mu_2)^2\beta^2)]$$

$$g_{336}=[9m^2-(\mu_1-2\mu_2)^2\beta^2]^2+\{K_1+K_2[9m^2-(\mu_1-2\mu_2)^2\beta^2]-9S_0m^2\}[1+\gamma(9m^2-(\mu_1-2\mu_2)^2\beta^2)]$$

$$g_{337}=81(m^2-\mu_1^2\beta^2)^2+[K_1-9S_0m^2][1+9\gamma(m^2-\mu_1^2\beta^2)]$$

$$g_{338}=81(m^2-\mu_2^2\beta^2)^2+[K_1-9S_0m^2][1+9\gamma(m^2-\mu_2^2\beta^2)] \tag{22}$$

Notations

a, b	plate length and breadth
D	flexural rigidity for a plate
E	elastic modulus for a plate
$\overline{F}$, F	stress function and its dimensionless form
G	in plane shear modulus for a plate
$\overline{K}_1$, K_1, k_1	Winkler elastic foundation stiffness and its two alternative dimensionless forms
$\overline{K}_2$, K_2, k_2	Pasternak elastic foundation stiffness and its two alternative dimensionless forms
$\overline{K}_3$, K_3, k_3	softening nonlinear elastic foundation stiffness and its two alternative dimensionless forms
t	thickness of a plate
$\overline{W}$, W	deflection of a plate and its dimensionless form
$\overline{W}^*$, W^*	geometrical imperfection of a plate and its dimensionless form
α	thermal expansion coefficient for a plate
β	aspect ratio of plate, $=a/b$
Δ_x, δ_x	end-shortening and its dimensionless form
ε	a small perturbation parameter
κ^2	shear factor for a moderately thick plate
λ_T	dimensionless form of thermal stress
μ	imperfection parameter
ν	Poisson's ratio
$\overline{\Psi}_x$, Ψ_x	rotation and its dimensionless form